ISTANBUL TECHNICAL UNIVERSITY ★ GRADUATE SCHOOL OF SCIENCE ENGINEERING AND TECHNOLOGY

HIGH FREQUENCY CHARACTERIZATION OF PRINTED AND ETCHED FABRIC BASED CONDUCTIVE MATERIALS FOR THE DEVELOPMENT OF WEARABLE ANTENNAS

M.Sc. THESIS

Toumaj KOHANDEL GARGARI

Department of Electronics and Telecommunication Engineering

Electronics Engineering Programme

Thesis Advisor: Assoc. Dr. Nil TARIM

OCTOBER 2012

ISTANBUL TECHNICAL UNIVERSITY ★ GRADUATE SCHOOL OF SCIENCE ENGINEERING AND TECHNOLOGY

HIGH FREQUENCY CHARACTERIZATION OF PRINTED AND ETCHED FABRIC BASED CONDUCTIVE MATERIALS FOR THE DEVELOPMENT OF WEARABLE ANTENNAS

M.Sc. THESIS

Toumaj KOHADEL GARGARI
(504091260)

Department of Electronics and Telecommunication Engineering

Electronics Engineering Programme

Thesis Advisor: Assoc. Dr. Nil TARIM

OCTOBER 2012

İSTANBUL TEKNİK ÜNİVERSİTESİ ★ FEN BİLİMLERİ ENSTİTÜSÜ

GİYİLEBİLİR ANTENLERIN GELİSTİİRİLMESİNDE KULLANILAN BASKILI VE OYMA KUMAŞ BAZLI İLETKEN MALZEMELERİN YÜKSEK FREKANS KARAKTERİZASYONU

YÜKSEK LİSANS TEZİ

Toumaj KOHANDEL GARGARİ
(504091260)

Elektoronik ve Haberleşme Mühendisliği Anabilim Dalı

Elektronik Mühendisliği Programı

Tez Danışmanı: Assoc. Dr. Nil TARIM

EKIM 2012

Toumaj KOHANDEL GARGARI, a **M.Sc.** student of ITU **Institute of / Graduate School of Electronics** student ID **504091260**, successfully defended the **thesis/dissertation** entitled "**HIGH FREQUENCY CHARACTERIZATION OF PRINTED AND ETCHED FABRIC BASED CONDUCTIVE MATERIALS FOR THE DEVELOPMENT OF WEARABLE ANTENNAS**", which he prepared after fulfilling the requirements specified in the associated legislations, before the jury whose signatures are below.

Thesis Advisor :   **Assoc. Dr. Nil TARIM**   ....
                       İstanbul Technical University

Jury Members :   **Assis. Dr. Serkan SIMSEK**   ....
                       İstanbul Technical University

                       Assis. Dr. Serhat IKIZOGLU   ....
                       İstanbul Technical University

Date of Submission : 22 June 2012
Date of Defense :   29 October 2012

To my parents,

FOREWORD

At the first, I would like to express my deep appreciation to Dr. Frederick Declercq for his endless efforts in educating me and of course leading me through this thesis.Via this thesis and his guidance, I have met new methods of research, new programs and this, provided me to obtain different experiences.

I would like to thank Prof. Dr. Hendrik Rogier, who has given me the precious opportunity to be participated in this scientific environment and also, complete cover and kind suggestions and support.

I thank Doc.Dr.Nil Tarim, my promoter in my home institution, for consultancy and comprehensive assistance during my MS.c.

Also, I would like to appreciate Prof. Dr. Osman Palamutcuogullari for motivating me, persistent support and giving me the viewpoint on RF microelectronics and Antennas .

June 2012   Toumaj KOHANDEL GARGARİ
                                                          Electronics Engineer

x

TABLE OF CONTENTS

ABBREVIATIONS

PCB	**:** Printed Circuit Board
ADS	**:** Advanced Design System
EM	**:** Electromagnetic
EMI	**:** Electromagnetic Interference
ISM	**:** Industrial Scientific and Medical
MoM	**:** Method of Moments
MP	**:** Matrix Pencil
MPA	**:** Microstrip Patch Antenna
RF	**:** Radio Frequency
SMA	**:** SubMiniature version A
SUMO	**:** SUrrogate MOdelling
TE	**:** Transverse Electric
TEM	**:** Transverse Electromagnetic
TM	**:** Transverse Magnetic
SBO	**:** Surrogate Based Optimization
BWA	**:** Body Wearable Antennas
GPS	**:** Global Positioning System
ADS	**:** Advance Design System
BW	**:** Bandwidth

LIST OF TABLES

LIST OF FIGURES

HIGH FREQUENCY CHARACTERIZATION OF PRINTED AND ETCHED FABRIC BASED CONDUCTIVE MATERIALS FOR THE DEVELOPMENT WEARABLE ANTENNAS

SUMMARY

Wearable textile system and its revolutionary emphasis on the world of electronics, telecommunication and textile has undisputable role in our daily life. The use of flexible electronics and wearable antenna are growing each day. Industrial and space related applications along with the medical, rescue affairs, cell phone and GPS are outstanding usage of these technologies.

A wearable antenna is applied to enable the communication in so-called wireless communication. These wearable antennas must be integrated easily in the cloth, comfortable and endurable to any bending or crumpling and in another word they have to be flexible.

This thesis is dedicated on the characterization methods of wearable antennas and microstrip lines at resonance frequency of 2.45GHz, ISM band. Primarily, the characterization approach is presented in order to determine the complex permittivity of the textile antenna substrate as well as the effective conductivity of the electrotextile. In this inverse technique, material parameters are extracted by comparing measured and simulated antenna results. Additionally, the inverse problem is solved using a surrogate-based optimization method as implemented in the SUrrogate MOdeling (SUMO) Toolbox, resulting in the quicker and more accurate determination of the electromagnetic properties in comparison of solving inverse problem of manually.

Another characterization method based on S-parameters measurements, is applied to a pair of microstrip lines with different lengths. De-embedding of the coax-to-microstrip line transitions obtained from measurements yields the complex propagation constant where permittivity and loss tangent can be extracted.

Finally, combination of the de-embedding method along with the surrogate-based optimization method are applied to a pair of microstrip lines in order to optimize their electromagnetic properties.

Consequently, usage of electrotextile as conductor material affects the effective permittivity of the substrate. So, textile substrate characterization for wearable antennas and microstrip lines demands same conductive materials used for them in order to test them. This research concentrates on development of wearable antennas and microstrip lines.

GİYİLEBİLİR ANTENLERİN GELİŞTİİRİLMESİNDE KULLANILAN BASKILI VE OYMA KUMAŞ BAZLI İLETKEN MALZEMELERİN YÜKSEK FREKANS KARAKTERİZASYONU

ÖZET

Elektronik, telekomünikasyon ve tekstil dünyasına Giyilebilir tekstil sistemi ve onun devrimci vurgusu günlük hayatımızda tartışılmaz bir rolü vardır. Esnek elektronik ve giyilebilir anten kullanımı her geçen gün büyüyor.Medikal, kurtarma işleri ile birlikte sanayi ve uzay ile ilgili uygulamalar, cep telefonu ve GPS, bu teknolojilerin olağanüstü kullanımlarındandir.

Giyilebilir tekstil sistemleri yeni bir araştırma alanıdır ve ortaya çıkması, Doksanlı yılların sonlarında ile ifade edilir. Bu gelişme bez bizi korur ama aynı zamanda bizim ikinci bir deri gibi fonksiyonları da içerir ve sadece bu bakış açısından kaynaklanmaktadır. Sensörler, bir veri işleme birimi, bir iletişim sistemi, bir enerji kaynağı ve bağlantıları gibi gösterilmiştir. adlandırılan giyilebilir tekstil sistemi, temelde altı parçadan oluşur. Sensörler vücut veya çevre ile ilgili bilgi sistemi sağlar. Bunlar sıcaklık, solunum ve kalp hızı, ya da nem, sıcaklık ve zehirli gazların varlığı gibi çevresel verilerin hissedebilir giysi dışında konumlandırılmış olarak bez algılama verileri entegre edilebilir.

Elde edilen veriler işlenmesi gerekir. Bu genellikle PCB üzerine monte edilmiş elektronik ile yapılır. Elektronik bileşenlerin esnek bir alt tabaka üzerine monte edilmiş esnek bir elektronik, giriş tekstil malzemeleri ile uyumluluğu arttırmaktadır.

Giysi ve harici baz istasyonu arasındaki iletişim kablosuz bir iletişim sistemi ile etkindir. Bir çalıştırıcı bir şey yanlış giderse takan uyaran bir işitsel veya görsel alarm olabilir. Gerekli enerji piller rahat bir şekilde giysi içine entegre edilebilen tercih edilen bir esnek olanlar tarafından sağlanmaktadır.Ara bağlantıları bütün sistemleri hep birlikte bağlamak için kullanmaktadır .

Bir giyilelabilir anten kablosuz iletişim içinde iletişimi sağlamak için uygulanır. Bu giyilebilir antenleri rahat ve dayanıklı kumaş, kolayca entegre edilmelidir herhangi bir eğilme veya buruşturma ve esnek olmak zorunda . Yani, giyilebilir anten tasarımı, esnek malzeme uygulanması fikrini ortaya çıkmıştır ve ilk tekstil anten inşa edilmişdir.

Çeşitli nem için tasarlanmış hafif ve esnek bir malzemeden yapılmış Giyilebilir antenler, ve tüm bunları giyen rahatsız olmayan üzerindeki en önemli çalışmaktır ve onları üretmek için bilim ve endüstri enteresan avantajları vardır.

Bu uygulamalarda Giyilebilir antenler alabora kurtarma grubu tarafından bulunmasını yardımcı hayat ceket içine dikilir. Başka bir uygulama olarak, itfaiyecinin giysinde uygulanabilir birbirleri ile ve merkezi kumanda istasyon ile iletişim kurmasına izin veren ya da bunu bir GPS olarak polis tarafından

kullanılabilir. Genel olarak, madencilik, petrol ve doğal gaz endüstrileri gibi tehlikeli meslek için yararlıdır.

Bu fenomen bir başka önemli uygulama cep telefonlarında yer almaktadır. Ayrıca, hafif ağırlığa sahip olan ve çevre ile uyumlu olması e-tekstil antenler çok geniş bir uygulama alanı olarak kullanılmaktadır.

Bu çalışmanın başlamasından yapılacak bunların düzeni elde etmek için Antenler ve mikroşerit hatlar simülasyonu dir. Simülasyon ADS Momentum bir ortamda gerçekleştirilir.

İlk olarak, simülasyon önce de 50 Ω satırın modelleme sağlamak için antenin besleme hattında (mikroşeritli hattı) genişliğini w_f hesaplamak gerekir. Bunu yapmak için, biz Linecalc, bir iletim hattı synthesizer aracını kullanın.

İkincisi, biz Azurri 3.4 mm ve pamuk 2,45 GHz ISM band rezonans frekansında 2.3 mm substrat için verilen geçirgenlik ve kayıp tanjant ve kalınlığı ile onları simule etmekdir.

Simülasyonu yapılır ve layoutlar elde etdikden sonra, ikinci adımı onları imal etmektir. Onları üretmek için herhangi bir özel ve modern ekipmanları ihtiyacı yoktur çünkü bu işin en ilginç kısmı bunları yapmaktır.

İlk olarak, bu lehim bağlantısı sonra kumaşlar ve kesilmiş iletken ve demir ısı ile yapışkan tabaka ile bir araya bağlamak ve. Şekil 4.3 'de, fabrikasyon antenler ve mikroşerit hatlar gösterilir

Bu tezde, 2.45GHz rezonans frekansında giyilebilir antenler ve mikroşerit hatlar ve karakterizasyon yöntemleri araştırılmaktadır. Öncelikle, karakterizasyon yaklaşım tekstil alt tabaka anten kompleks permitivitelerinin hem de electrotextile etkin bir iletkenlik tespit etmek için sunulmuştur. Bu ters tekniği, malzeme parametreleri ölçülen ve simüle anten sonuçları karşılaştırılarak elde edilmiştir. Ayrıca, ters problem elle ters problem çözme karşılaştırması elektromanyetik özellikleri daha hızlı ve daha doğru Surrogate Model (SUMO) Toolbox, uygulanan gibi bir vekil tabanlı optimizasyon yöntemi kullanılarak çözülmüştür.

S-parametrelerinin ölçümlere dayanan bir tanımlama yöntemi, farklı uzunlukta olan bir çift mikroşeritli çizgiler de uygulanır. Geçirgenlik ve kayıp tanjantı ekstrakte edilebilir nerede ölçümlerden elde coaxial-to-microstripline hat geçişleri De-embedding kompleks yayılma sabiti verir.

Son olarak, ilk kez için, taşıyıcı tabanlı optimizasyon yöntemi ile birlikte de gömme yöntemi kombinasyon ancak daha ileri bir alt tabaka olarak iki malzemenin üzerine elektromanyetik özelliklerin optimize edilmesi için, farklı uzunlukta mikroşeritli çizgiler bir çift uygulanan Daha fazla malzeme araştırmalarının kapsamlı bir sonuç sonucuna nedeniyle gereklidir.

Bu araştırmanın nihai hedefi giyilebilir antenler ve mikroşerit hatlar geliştirme amacıyla electrotextile esaslı iletken malzemelerin elektromanyetik özellikleri karakterize etmek oldu. Ters anten sorunu ve mikroşerit hatlar için uygulanan De-embedding yöntemi iki kullanılan yöntemdir.

Ters anten sorunu çalışmada,yöntem yüzeylerde pamuk ve Azurri iki tür substrat olarak uygulanır. Iletken kayıpları ve substrat kayıplar arasındaki ayrım üzerinde kaçınılmazlığı nedeniyle, bakır ve Flectron kayıpları ayrıyoruz.Bu yöntemle, daha istikrarlı iletkenlik pamuk bazlı antenler ulaştı.

Her bir antenin beş numune üzerinde bu yöntemini icra etmek sayesinde, sonuçlar tekrarlanabilirliği incelenmiştir.De-emdedding yöntemi çalışmada,Substrat olduğu ve bağıl dielektrik kayıp tanjantı hesaplanabilir ki farklı uzunluklarda iki mikroşerit hatlar üzerindeki yöntemi uygulamak ideal kayıplı iletim hattı sürekli karmaşık yayılımı ayıklanır.De-embedding ve SBÖ çalışma birleşik bir yöntem olarak,De-embedding optimum noktaları elde etmek için SUMO Toolbox uygulanan vekil tabanlı optimizasyon ile birlikte ölçülen ve simüle edilen veriler için uygulanır.

Bu antenler ve aynı miktar içinde aynı malzemeler için yapılır. Ayrıca, electrotextile mikroşeritli çizgilerinin elde edilmesi iki anten gibi olarak katlanır.Pamuk bazlı mikroşerit hatlar ve anten sonuçları arasındaki geçirgenlik, kayıp tanjantı ve iletkenlik arasında da benzerlikler vardır.Diğer taraftan, Azurri tabanlı mikroşerit hatlar ve antenler arasında, sadece geçirgenlik değerleri nispeten benzer ve kaybı oldukça büyük bir tutarsızlık geçirgenlik değerleri. Azurri tabanlı mikroşerit hatlar arasında iletkenlik aralığında kararsızlık göre Azurri antenlerden daha fazladır.

Bu tezde, Ters anten sorunu sadece iki malzeme pamuk ve Azurri üzerinde gerçekleştirilir. Diğer kumaşlar üzerinde çalışmalar yapılabilir.Ayrıca, de-embedding yöntemiyle yapılabilir kumaş ve farklı kumaşlar üzerinde çalışmalar sadece iki tür malzeme üzerinde yapılmıştır.

De-embedding yöntemi ve SBÖ sonuçlarının kombinasyonu bazı sapmalar olması ve halen daha fazla anten muadili ile benzer sonuçlar elde etmek için, üzerinde yapılması gereken daha fazla kesinlik önlemler gereklidir.Bu arada, ikinci yöntem substrat olarak değişik kumaşların değişik mikroşeritler üzerinde gerçekleştirilebilir.

Tezin sırası gelince, Bölüm 2 ve 3 mikroşerit hat ve mikroşerit yama anten hakkında genel bilgiler endişe duymaktadır. Bölüm 4 Bölüm 5 Bu çalışmanın temel amacı tanımlayan bu Araştırmada uygulanan pratik meseleleri üzerine adamıştır, mikroşerit hatlar ve mikroşerit yama anten karakterizasyon yöntemleri. Son olarak, Bölüm 6 iki mikroşerit hatlar üzerinde uygulanan yeni kombine karakterizasyon yöntemi açıklar. Yolun sonunda, sonuçlar ve gelecekteki iş tanımları vardır.

1. INTRODUCTION

The emergence of a new research field, of *wearable textile systems* is referred to the late nineties [1]. This development arises from the viewpoint that the cloth not only protects us but also functions as our second skin. A so-called wearable textile system basically consists of six components: sensors, actuators, a data processing unit, a communication system, an energy supply and interconnections, as depicted in the Figure 1.1. Sensors provide the system with information regarding the body or environment. They can be integrated in the cloth sensing data such as temperature, respiration and heart rate, or positioned on the outside of the garment where they sense environmental data such as humidity, temperature and presence of toxic gases.
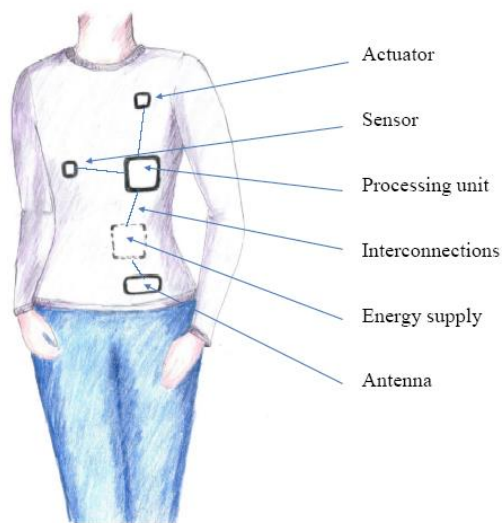
Figure 1.1: Components of a wearable textile system [2].

The gathered data need to be processed. This is done with electronics that are commonly assembled on PCBs. The introduction of flexible electronics, where the electronic components are mounted on a flexible substrate as shown in Figure 1.2, enhances the compatibility with textile materials.

Figure 1.2: Flexible electronics for integration in a wearable textile system [3].

The communication between the garment and an external base station is enabled with a wireless communication system. An actuator could be an audial or visual alarm that warns the wearer if something goes wrong. Required energy is provided by batteries, preferable flexible ones that can be integrated into the garment in a comfortable way. The interconnections connect the whole systems all together [2].

A wearable antenna is applied to enable the communication in so-called wireless communication. These wearable antennas must be integrated easily in the cloth, comfortable and endurable to any bending or crumpling and in another word they have to be flexible. So, the idea of applying flexible material in wearable antenna design has emerged and first textile antenna constructed [4].

Wearable antennas, made from light weighted and flexible material designed for various humidity [5] and the most important of all non–bothering in wearing them are the advantages that attract scientist and industry to work on and produce them [3].

Wearable antennas in these applications are sewn into the life jacket helping the shipwrecked to be found by rescue group. As another application ,it can be applied in the garment of the firefighter [5] allowing to communicate with each other and with the central command station or it can be used by police officers as a GPS [7]. Generally, it is useful for the hazardous occupations like mining, oil, natural gas industries, indeed.

Another important application of this phenomenon is in the cell phones .Also, E-textile antennas having light weights and being adaptable by the environment are very wide used in space application [8]. Effectively, wearable antennas being jack-of-all-trades, made a splash in the world of technology.

In this thesis, the characterization methods of wearable antennas and microstrip lines at resonance frequency of 2.45GHz is being researched. Primarily, the characterization approach is presented in order to determine the complex permittivity of the textile antenna substrate as well as the effective conductivity of the electrotextile. In this inverse technique, material parameters are extracted by comparing measured and simulated antenna results. Additionally, the inverse problem is solved using a surrogate-based optimization method as implemented in the SUrrogate MOdeling (SUMO) Toolbox, resulting in the quicker and more accurate determination of the electromagnetic properties in comparison of solving inverse problem manually.

Another characterization method based on S-parameters measurements, is applied to a pair of microstrip lines with different lengths. De-embedding of the coax-to-microstrip line transitions obtained from measurements yields the complex propagation constant where permittivity and loss tangent can be extracted.

Finally, for the very first time, combination of the de-embedding method along with the surrogate-based optimization method are applied to a pair of microstrip lines of different length, in order to optimize their electromagnetic properties on two materials as the substrate however further research on more materials is needed due to conclude in a comprehensive result.

As for the order of the thesis, Chapters 2 and 3 is concerned on general information on microstrip line and microstrip patch antenna. Chapter 4 is dedicated on the practical affairs applied in this research where Chapter 5 describes the main goal of this work, characterization methods of microstrip lines and microstrip patch antenna. Finally, Chapter 6 explains novel combined characterization method applied on the two microstrip lines. At the end of the road, there are conclusions and future work descriptions.

2. MICROSTRIP LINE

A microstrip line is a kind of transmission line used to deliver signals and consisting of a conducting strip and ground plane of same material separated by a dielectric layer called substrate. A microstrip line is shown in Figure 2.1 and characterized by propagation constant, characteristic impedance and a length.

Microstrip line in Figure 2.1 has a length *L* and *W*. Also, T stands for the thickness of the strip. H stands for Height.
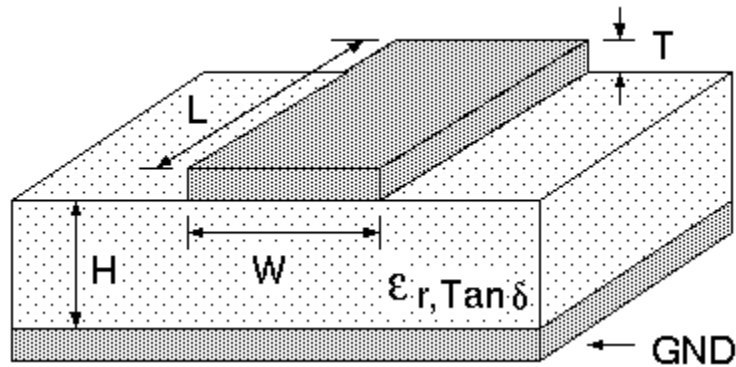
Figure 2.1: Microstrip line cross section [17].

2.1 Required Definitions

Before discussing microstrip lines, we have to focus on some vital definitions.

ε_r**:** *Relative Permittivity or Dielectric constant*

Permit of dielectric material to be affected by electric field relative to that in a vacuum or air is called relative permittivity.

$\varepsilon_{r,eff}$ *Effective permittivity or Effective dielectric constant*

Due to part of the fields from the microstrip conductor exist in air, the relative effective dielectric constant $\varepsilon_{r,eff}$ is somewhat less than the substrate's dielectric constant (also known as the relative permittivity). Relationship between them is:

$$1 < \varepsilon_{r,eff} < \varepsilon_r \qquad\qquad (2.1)$$

It is also important to mention that $\varepsilon_{r,eff}$ is related to height, width, relative permittivity and resonance frequency.

Complex permittivity

Generally, fabrics and foams applied in the textile antenna and microstrip lime design are lossy yielding a complex permittivity as:

$$\varepsilon = \varepsilon' - j\varepsilon'' = \varepsilon_0 \varepsilon_r (1 - j\tan\delta) \qquad\qquad (2.2)$$

Where ε', ε'' respresent the real and imaginary part of the permittivity, respectively, and $\tan\delta = \dfrac{\varepsilon''}{\varepsilon'}$, ε_r is relative permittivity and ε_0 is free space permittivity.

tanδ: Loss Tangent

The loss tangent is dielectric material`s inherent dissipation of electromagnetic energy.

μ: Permeability

In electromagnetic, permeability is the measure of the ability of a material to support the formation of a magnetic field within itself.

σ: Conductivity

In electromagnetic, the material`s ability to conduct the electromagnetic signal.

2.2 S-parameters (Scattering Matrix)

The relationship between input and output ports (terminals) are described by S-parameters. If we have two ports as in Figure 2.2, we will get S_{11}, S_{12}, S_{21} and S_{22}, where S_{12} represents the power transferred from port 1 to port 2, S_{21} represents the power transferred from port 2 to port 1.The most commonly used S-parameter in antenna design is S_{11} which represents reflection coefficient from port 1 and so S_{22} from port 2 [7].
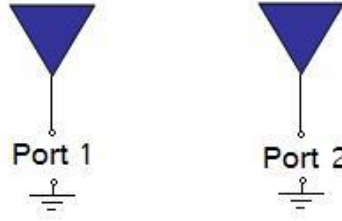
Figure 2.2: two-port network.

The relationship between the reflected power waves b_2, b_1, incident power waves a_1, a_2 and the S-parameter matrix is given by [15]:

.

$$\begin{pmatrix} b_1 \\ b_2 \end{pmatrix} = \begin{pmatrix} S_{11} & S_{12} \\ S_{21} & S_{22} \end{pmatrix} \begin{pmatrix} a_1 \\ a_2 \end{pmatrix}$$
(**2.3**)

The definitions of b_2, b_1, a_1, a_2 are depicted in Figure 3.3:

Figure 2.3: b_2, b_1, a_1, a_2 depiction.

Expanding the matrices into equations gives:

$$b_1 = S_{11} a_1 + S_{12} a_2$$
(**2.4**)

$$b_2 = S_{21} a_1 + S_{22} a_2$$
(**2.5**)

(3.4), (3,5) give the relationship between reflected and incident power waves at each of the network ports, 1 and 2, in terms of the network's individual S-parameters, S_{11}, S_{12}, S_{21} and S_{22}. However if, according to the definition of S-parameters, port 2 is

7

terminated in a load identical to the system impedance (Z_0) then, b_2 will be totally absorbed making a_2 equal to zero. Therefore [19]:

$$S_{11} = \frac{b_1}{a_1} \text{ when } a_2=0 \quad \text{and} \quad S_{21} = \frac{b_2}{a_1} \text{ when } a_2=0 \tag{2.6}$$

Similarly, if port 1 is terminated in the system impedance then a_1 becomes zero, giving

$$S_{12} = \frac{b_1}{a_2} \text{ when } a_1=0 \quad \text{and} \quad S_{22} = \frac{b_2}{a_2} \text{ when } a_1=0 \tag{2.7}$$

2.3 Propagation Constant

The propagation constant is an important parameter associated with transmission lines, particularly microstrip lines. It is a complex number denoted by Greek letter γ (gamma), and is used to describe the propagation of an electromagnetic wave along a transmission line. [17]

The propagation constant γ consists of two parts which have diverse emphasis on signal propagation;

$$\gamma = \alpha + j\beta \tag{2.8}$$

The real part α of the propagation constant is the attenuation constant and it causes the signal amplitude to decrease along a transmission line. The imaginary component β of the propagation constant is phase constant which determines the speed of propagation and phase variation of the signal along the transmission line.

.

3. MICROSTRIP PATCH ANTENNA

A Microstrip Patch Antenna (MPA) is a planar antenna with increasingly useful applications due to the capability of being printed directly on the circuit board. Such antennas have a thin profile, light weighted, easy to fabricate, low cost, relatively compact dimension and of course compatibility with electronic circuits, are some advantages which make MPA favorite in the medical, industry and space (aircraft) applications and they became widespread for mobile equipment, too [7].On the other hand, narrow BandWidth ($\approx$3%) [10], somewhat low gain (6 dB) and parasitic radiation by feed lines are some disadvantages of MPA`s. Consider a MPA in Figure 3.1; A microstrip antenna is a conductive patch of ($L*W$) on top of a dielectric material with the height of h known as the substrate that both sit on top of a ground plane which is constructed from the same material as for patch. It is a merit to mention that height of the substrate is much smaller that the wavelength but not smaller than $h = 0.05\lambda$, and the length L is of the order of 0.5λ. The relation between W and L satisfies *1<W/L<2* [11].
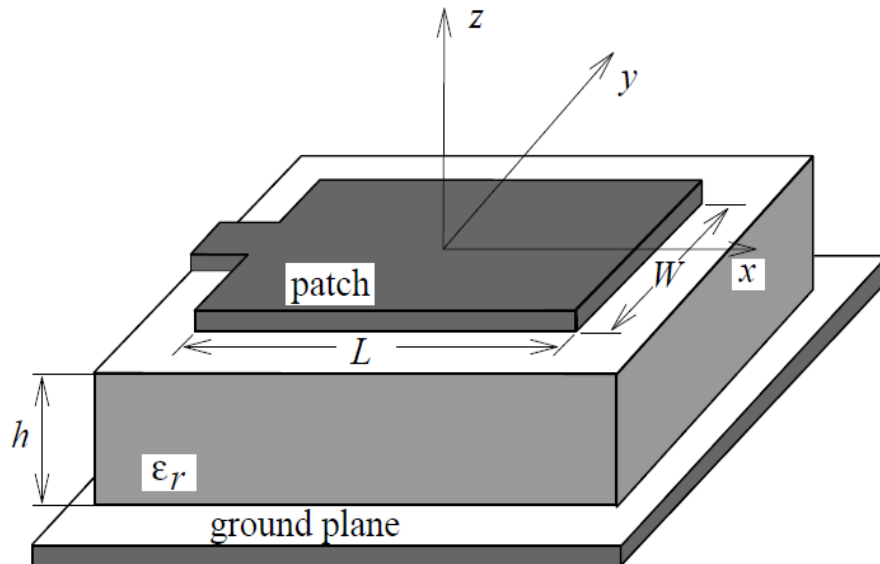
Figure 3.1: Microstrip Patch Antenna (MPA) [7].

Resonance frequency is determined by the length L and will be defined as:

$$f \approx \frac{c_0}{2L\sqrt{\varepsilon_r}} \qquad (3.1)$$

Where c_0 is free space speed of light, ε_r is relative permittivity of substrate that originated from the effective permittivity. Also, in order to achieve resonance, one should have L half of the wavelength:

$$L = \frac{\lambda_o}{2} = \frac{\lambda}{2\sqrt{\varepsilon_{r,eff}}} \qquad (3.2)$$

Where λ_o being the free space wavelength and λ is the wavelength in the substrate .

3.1 Feeding

Various feeding techniques for stimulating the patch antenna exist e.g. edge-feeding, inset-feeding, coaxial-probe feeding, aperture -coupled feeding. The feeding technique used in this research, is inset-feeding shown in Figure 3.2:
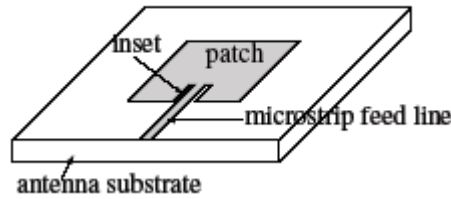
Figure 3.2: Microstrip patch antenna with inset feed [3].

3.2 Substrate

Selecting an appropriate substrate with the height h is of vital importance in patch antenna design due to the properties of relative permittivity ε_r, loss tangent $\tan\delta$.Fellow antennas get better antenna efficiency with lower permittivity and a low loss tangent is the source of low dielectric losses of the substrate. Also, thicker substrate gives higher antenna efficiency. Therefore, in order to have high antenna efficiency, we would like to have relatively thick substrate with small permittivity and small loss tangent [3]. The substrates have been used in this research are Azurri and cotton.

3.3 Characteristics

In this part, we review some characteristics of an antenna which is the most necessary part of a radio communicational system which has the prominent role of sending and/or receiving of the electromagnetic waves. Creating a radio communicational system demands knowing how much antenna power is radiated from one antenna is in the distance R, $(R > \frac{2d^2}{\lambda})$ of another and how much power is received at the receiving point (3.3), where d is the largest dimension of the antenna and λ is the wavelength, so they are in each other`s far-field or Fraunhofer region.

Friis formula also called link budget satisfies:

$$\frac{P_r}{P_{t,max}} = M_r G_r(-u^i) L^{-1} Q_{rt}\left(u^i\right) G_t(u^i) M_t \tag{3.3}$$

Which P_r is the radiated power, $P_{t,max}$ maximum transmitted power, M_r, M_t, G_r, G_t are mismatch factors and power gains of received and transmitted antenna ,respectively and Q_{rt} represents the polarization between two antennas, $L = (\frac{4\pi R}{\lambda_0})^2$ free space path loss and u^i is the unit vector looking from receiving antenna to transmitting antenna. Having the background knowledge that wavefronts radiation takes place spherically and the path loss diminishes by R^2 there is nothing to do with the free space loss so as a tradeoff we work on improving the mismatch factor, gain and polarization to yield optimal link budget [7].

3.3.1 Input impedance
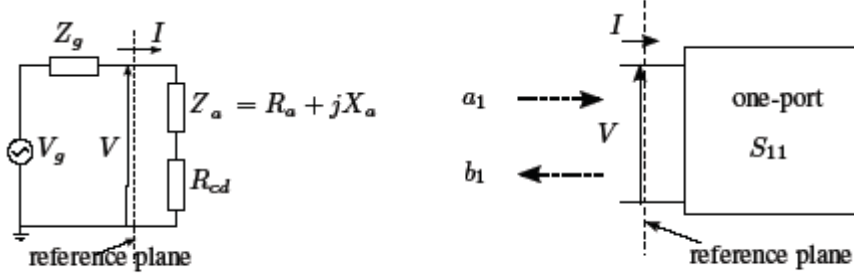
Figure 3.3: (a) Equivalent circuit of transmitting antenna (b) one-port S-parameter representation [5].

Figure 3.3 (a), demonstrates the equivalent circuit of a transmitting antenna with Z_g representing the impedance of the generator , V_g is the voltage of the generator , Z_{in} is the input impedance and R_{cd} models the conductor dielectric losses of the antenna. The reference plane separates antenna and generator from each other. So, the input impedance is:

$$Z_{in} = \frac{V}{I} = Z_a + R_{cd} = R_a + jX_a + R_{cd} \tag{3.4}$$

Which Z_a is antenna radiation impedance, R_a is the resistance of antenna related to the far field behavior of antenna and X_a shows the reactance of antenna related to the near field antenna behavior. Hence, the power transmitted to the antenna can be calculated from:

$$P_T = M \, P_{max} \tag{3.5}$$

Where P_{max} is the maximum power that the generator can deliver to the antenna and M is mismatch factor. Maximum power transfer is obtained when conjugate complex value of generator impedance is equal to the input impedance. Matching condition arises from this condition and in microwave circuit design is 50Ω.

The reflection coefficient is:

$$\Gamma = \frac{Zin - Zg}{Zin + Zg} \tag{3.6}$$

And mismatch factor is:

$$M = 1 - |\Gamma|^2 \tag{3.7}$$

12

Hence, maximum power transfer occurs when *Γ=0 and M= 1*. [5]

In the effort of high frequency measuring by means of network analyzer, we use the term reflection coefficient Γ to be equal to the S-parameter, S_{11}. In a one-port network like the antenna, the incident wave and reflected wave have the relation following:

$$S_{11} = \frac{b_1}{a_1} \qquad (3.8)$$

Throughout this work we use the term $|S_{11}|$ as for the decibel value of S_{11} representing the logarithmic value of that which is $20\log|S_{11}|$ hence, we are trying to achieve the $|S_{11}| < -10$dB denotes that 90 % of the power is injected into the antenna and just 10 % is reflected back toward the generator[8].

It is a merit to remember that there is a inverse relation between bandwidth *BW* and quality factor *Q* at the frequency of resonance. As we know the quality factor is an important element which gives us important information on amount of energy stored *W* in the antenna over the loss of power *P*. Losses are divided to four groups of losses; conductor conductivity, dielectric conductivity (dielectric loss tangent), surface waves and radiation loss [8].

$$BW \sim \frac{1}{Quality\ Factor} \qquad (3.9)$$

$$Quality\ Factor \sim \frac{Stored\ Energy}{Power\ loss} \qquad (3.10)$$

By minimizing the amount of power losses (*P*), quality factor decreases and also, using a thick substrate increases the losses and results in the decreased quality factor.

3.3.2 Radiation pattern and directivity

Radiation pattern is the variation of the radiated power as a function of direction away from the antenna. In the Figure 3.4, you can see an example of radiation pattern of an antenna. In this example, radiation in the x-y plane is maximum though it is minimum in the direction of z. Radiation pattern is useful to determine which directions antenna radiates.
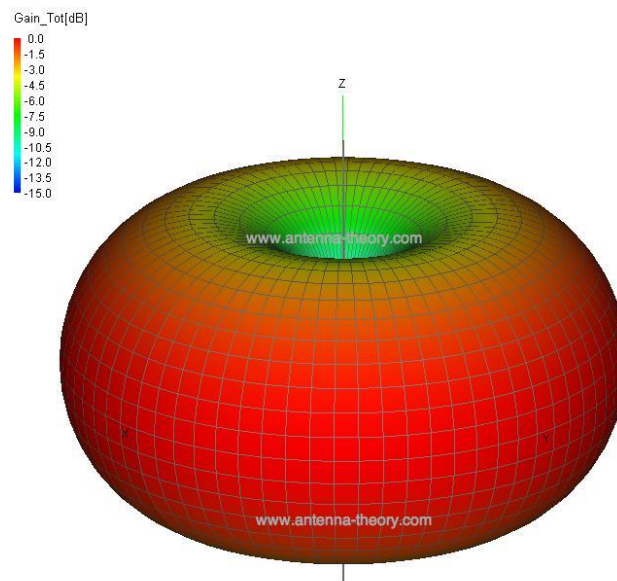
Figure 3.4: Radiation Pattern [12].

Directivity the how directional radiation pattern of antenna is. In other words, the maximum value of radiated power over average and the result is directivity. For instance omnidirectional antenna would have 1 or 0 dB directivity and for patch antenna directivity is 3.2-6.3 or 5-8 dB. [10]

In reality, cell phone antennas must have low directivity because they have to receive/transmit from any direction but satellite dishes must have high directivity due to the fixed direction of receiving signals and long distance between them.

3.3.3 Efficiency and gain

Clearly, the most important property of an antenna is its radiation efficiency, which is defined as:

$$e_{cd} = \frac{P_{rad}}{P_{tot}} \tag{3.11}$$

where P_{rad}, P_{tot} are radiated power and total power, respectively.

and

$$P_{tot} = (R_a + R_{cd}) \frac{|I_t|^2}{2} \tag{3.12}$$

which I_t is showing current in transmit or receive mode;

$$P_{rad} = R_a \frac{|I_t|^2}{2} \tag{3.13}$$

and by substituting (2.12), (2.13) into the (2.11) we can write:

$$e_{cd} = \frac{P_{rad}}{P_{tot}} = \frac{R_a}{R_a + R_{cd}} \tag{3.14}$$

and total efficiency is :

$$e_{tot} = \frac{P_{rad}}{P_{tot,max}} = M e_{cd} = (1 - |\Gamma|^2) \frac{R_a}{R_a + R_{cd}} \tag{3.15}$$

There are several methods to measure antenna efficiency like the radiation pattern method or the method where efficiency is measured applying directivity and gain of the antenna and then extracting the efficiency from that:

$$G(\theta, \varphi) = e_{cd} D(\theta, \varphi) \tag{3.16}$$

But the method we have used in our work is Generalized Wheeler Cap Method [14].

3.3.3.1 Generalized Wheeler cap method

The main advantage of using this method is its fast and easy applicability in comparison with other methods [14]. This method of measuring antenna efficiency is a technique which measuring efficiency requires two measurements of the input impedance [15]. First measurement takes place in free space where the second measurement is the antenna inside a metallic cavity [13]. The question here is that whether the near field and losses behaves the same with and without the cap and Wheeler`s answer was that having spherical cap of $\lambda/2\pi$ in radius would not disturb the near field [20].

So, input impedance of the desired antenna is measured at the frequency of resonance with and without cap. If the measured real part of input impedance without cap (free space) is R_1 and with the cap is R_2 then:

$$\eta = \frac{R_1 - R_2}{R_1} = \frac{R_r}{R_r - R_l} \tag{3.17}$$

Where R_r represents radiation resistance and R_l is loss resistance (including all losses of tuning and matching network losses) and η representing any two port network efficiency and equals e_{cd}. The role of the cap is to short circuit the radiation resistance and allowing R_l to be separated from R_r. So, by using the cap over antenna we obtain R_2 and we obtain R_1 while measuring in the free space, finally we put them in the (3.17) and we get antenna efficiency [18].

3.3.3.2 Measurements

For this experiment, we fabricated twelve antennas; half of this twelve is constructed with Azzuri as a substrate which conductive layer of one is copper and other five are Flectron. Another half, are from cotton where one of them containing the copper as a conductive layer and other five are out of Flectron. According to the Generalized Wheeler method , primarily we put the antenna on the ground plane and connect it to the network analyzer of Agilent Technologies Figure 3.5 which is calibrated earlier by means of calibration tool using an Agilent`s Electronic Calibration Module as shown in the Figure 3.6.

Figure 3.5: Network analyzer and calibrator

Figure 3.6: Calibrator

Afterwards, we connect all antennas to measure reflection coefficient in free space. Next, we place the antenna under test on a conductive ground plane as shown in the Figure 3.7 and fix it using adhesive tape to ensure that the antenna stays in place after positioning the metallic cavity over the antenna. Figure 3.8 shows a cavity over antenna. The antennas are centered in the middle of the circular cavity. In order to keep distance between antenna and cavity wall equally, the cavity is fixed by using a heavy weight as depicted in Figure 3.9, to make sure that the cavity and ground plane are properly connected. This applied circular cavity is big one with the diameter 0f

18 cm, we re-do this work for smaller circular cavity of *15cm* in diameter.We repeat these instructions for all of the twelve antennas.
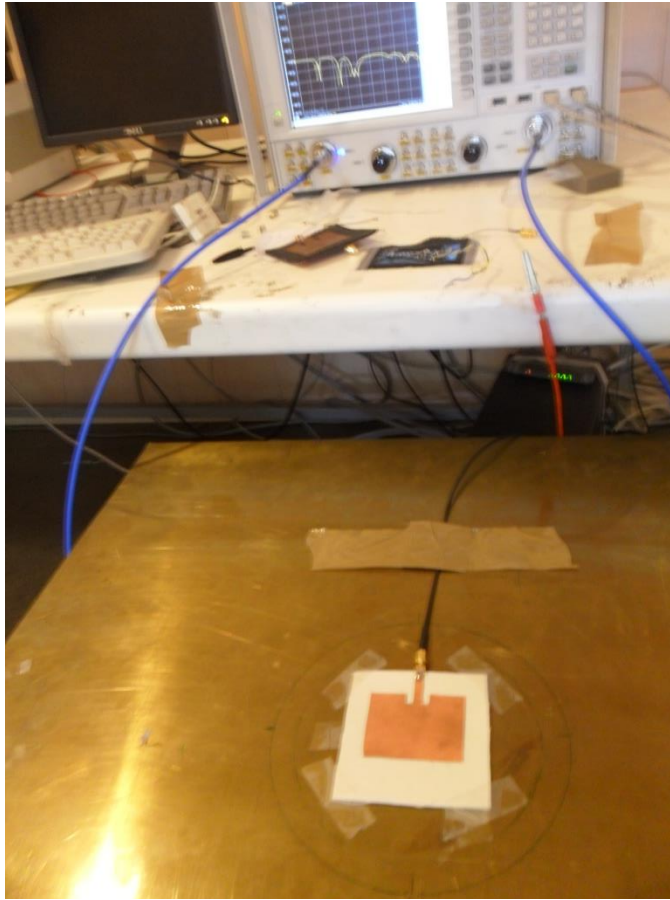
Figure 3.7: Antenna on ground plane in the center of circle

Using implemented script of this method in MATLAB where inputs of the script are measured S-parameters and the output is antenna efficiency is the next step. Figure 3.10(a) and Figure 3.10(b) depict results obtained from the large and small cavity, respectively, for antenna efficiency results of a sample antenna of cotton_Flectron in the frequency range of 2 GHz -3GHz. According to wheelers explanation, size and shape of the cap may be chosen different but the antenna efficiency is almost the same at the frequency of resonance as long as the distribution (near field) on the patch is not disturbed [19].

Figure 3.8: Placing cavity on the antenna

Figure 3.9: Placing the weight on the cavity
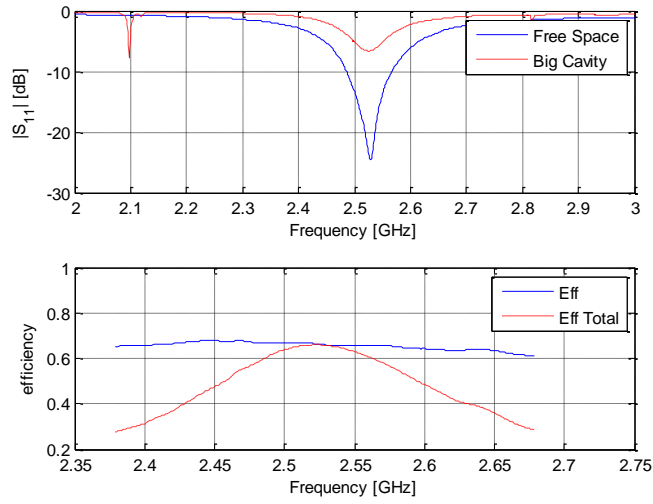
(a)Big Cavity
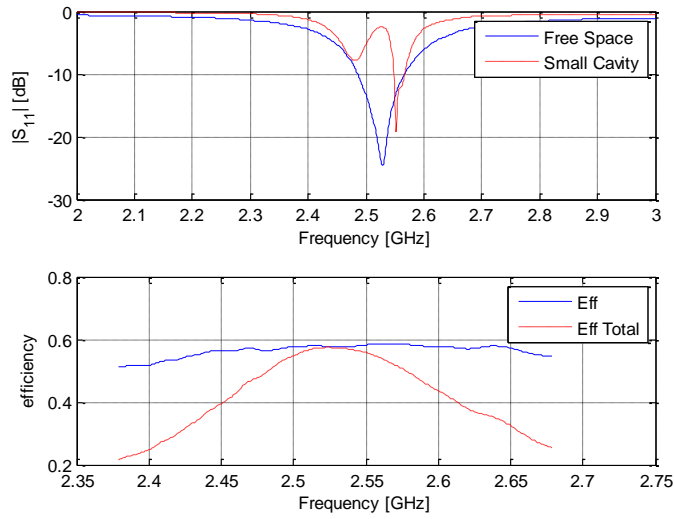
(b)Small Cavity

Figure 3.10: Generalized wheeler cap method applied for the cotton antennas using Flectron for conductive plane, (a) Big Cavity, (b) Small Cavity

4. SIMULATION AND FABRICATION

Commencement of this work was simulation of Antennas and Microstrip lines to obtain the layouts of them to be made. Simulation is performed in the Momentum environment of ADS as depicted in Figure 4.1.

Firstly, before simulation we have to calculate the width w_f of the feed line of the antenna (w_f of the microstrip line) to ensure modeling of the line at 50 Ω. In order to do this, we use Linecalc , a transmission line synthesizer tool.

Secondly, we simulate them with the given permittivity and loss tangent and the thickness for the substrate for Azurri 3.4 mm and cotton 2.3 mm at the resonance frequency of 2.45 GHz ISM band.
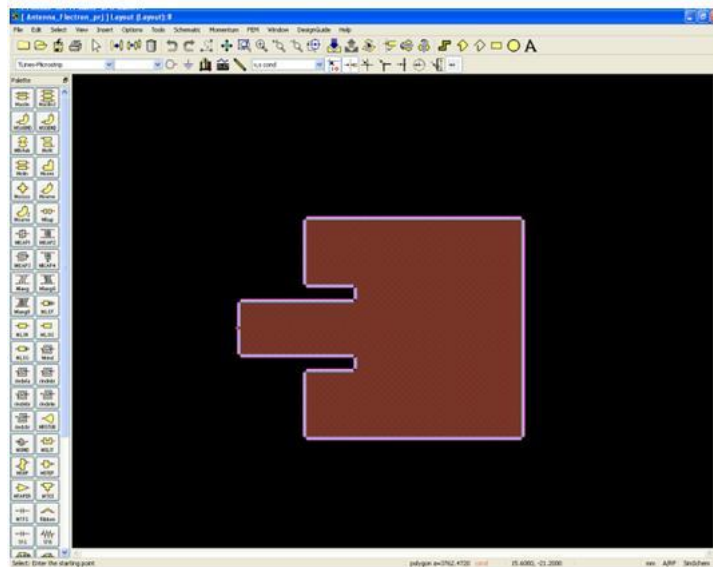
Figure 4.1: Momentum environment of ADS.

After the simulation is done and we have got the layouts, the second step is to fabricate them .The most interesting part of this work is making them because it does not need any special and modern equipments to fabricate them. All the materials and tools you need are:

- Fabrics: cotton, Azzuri, Conductors: copper, Flectron,Adhesive Sheet,Scissor,Iron,Soldering Tool and Solder,SMA Connector,Cutter,Caliper

as depicted in the Figure 4.2.

Figure 4.2: Materials and Tools.

Firstly, we cut the fabrics and conductors and attach them together with adhesive sheet by means of the heat of the iron and then we solder the connector. In Figure 4.3, fabricated antennas and microstrip lines are shown.

(a)
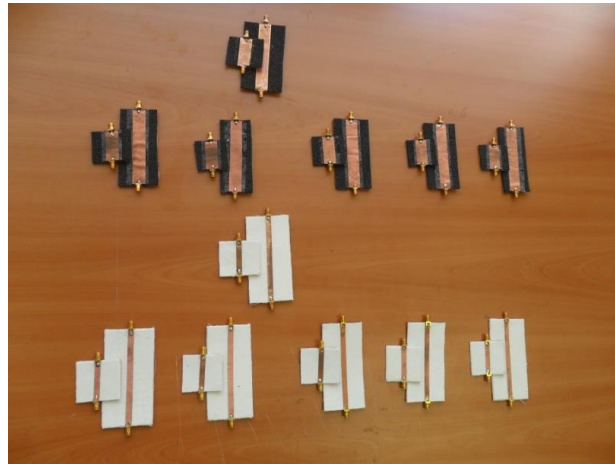
(b)

Figure 4.3: Fabricated antennas (a) and microstrip lines (b).

List of fabrication is:

-A cotton-Copper antenna, five cotton- Flectron antenna

-An Azzuri-copper antenna, five Azzuri- Flectron antenna

-A cotton-copper Microstrip line, five cotton- Flectron Microstrip lines of 100mm, 40mm

-An Azurri-copper Microstrip line, five Azurri- Flectron Microstrip lines of 100mm, 40mm

In Table 4.1 and Table 4.2 the dimensions of the fabricated antennas are given and in Table 4.3 and Table 4.4 dimensions of the fabricated microstrip lines are shown in millimeters as for unit, respectively. Figure 4.4 depicts the geometry of the antenna.
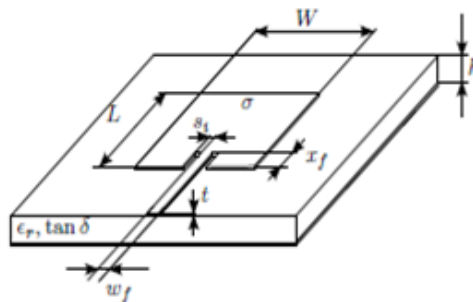
Figure 4.4: MPA`s dimensions identification.

Table 4.1: Copper based antenna dimensions

Copper	L	W	Lf	xf	si	wf	gnd
Cotton	44.79	59.68	24.52	5.88	3.78	6.26	99*91
Azurri	53.34	60.48	26.32	12.97	4.13	15.41	91*99

Table 4.2: Flectron based antenna dimensions

Flectron	L	W	Lf	xf	si	wf	gnd
Cotton1	46.06	60.13	24.21	6.87	4.08	5.77	90*90
Cotton2	44	58.89	24.72	6.31	4.6	6.43	83*84
Cotton3	45.8	60.98	26	6.61	4.1	6.1	95*91
Cotton4	46.14	59.85	23.54	6.74	4.23	6.25	95*98
Cotton5	45.32	60.05	23.74	6.64	4.45	5.92	94*91
Azurri1	54.85	69.57	26.54	13.77	4.06	15.64	84*78
Azurri2	55.02	59.96	25.28	14.09	3.67	16.05	92*92
Azurri3	54.28	60.99	24.87	13.32	3.92	16.41	96*98
Azurri4	54.07	61	26.55	13.57	3.65	16.19	97*96
Azurri5	52.69	59.61	24.92	13.51	3.97	45.65	95*92

Table 4.3: Copper based microstrip line dimensions

| Copper	L(Long/Short)	wf(Long/Short)	gnd(Long/Short)
Cotton	107.68/41.78	6.65/6.91	110.06*54.45/44.19*49.69
Azurri	98.94/40.03	16.16/16.17	100.23*55.46/42.05*47.76

Table 4.4: Flectron based microstrip line dimensions

Flectron	L(Long/Short)	wf(Long/Short)	gnd(Long/Short)
Cotton1	106.36/42.87	7.15/6.62	109.38*54.03/44.35*46.75
Cotton2	108.19/41.61	6.54/6.21	110.38*51.84/43.79*48.27
Cotton3	106.10/42.75	6.35/6.48	108.13*52.84/44.46*47.17
Cotton4	99.80/40.74	6.18/6.53	101.33*52.13/42.85*48.49
Cotton5	105.35/40.16	6.66/6.26	106.41*52.23/42.34*45.17
Azurri1	97.07/36.23	15.99/15.37	103.98*39.91/38.34*43.62
Azurri2	97.25/36.54	15.21/15.66	98.18*46.21/39.01*40.52
Azurri3	96.44/38.12	16.34/15.94	99.96*50.21/40.87*44.18
Azurri4	96.15/37.74	15.33/15.48	99.14*43.55/40.53*46.67
Azurri5	96.04/37.21	15.18/15.56	98.99*39.17/39.92*39.66

*Milimetric unit is used to show figures.

5. APPLIED METHODS FOR ELECTROMAGNETIC CHARACTERIZATION

In this work, two characterization methods are used. First one is de-embedding of two microstrip lines and second one is inverse antenna problem. First method also known as a broad band method is based on the S-parameters measurements of two microstrip lines with different length where complex propagation constant extracted from the de-embedding of coax-to-microstrip line and permittivity and loss tangent can be calculated from this measurement value.

Second method is inverse antenna method known as small band technique. In this technique, complex permittivity of the substrate and conductivity of the electrotextile are calculated by comparison between simulated and measured antenna data. Inverse problem is converted to the forward optimization process by minimizing an error function. Realization of this method is performed by using the surrogate-based optimization technique for minimizing the error function and extracting the unknown electromagnetic properties. This method has two steps. Firstly, optimization process is performed on textile antenna with copper conductive material which results in finding the permittivity and loss tangent of the substrate. Secondly, optimization process is performed on electrotextile based textile antenna where yields in effective conductivity of the substrate.

5.1 De-Embedding Of Two Microstrip Lines

In this thesis, the necessary steps for constructing an end-to-end streamflow forecasting system were discussed. These steps include the use One of the characterization methods used in this research is the de-embedding method. This broadband technique is based on the S-parameters (Scattering parameters) analyses applied to two microstrip lines with different lengths. This method enables us of measuring the propagation constant γ and extracting dielectric properties of the substrate such as permittivity and loss tangent of microstrip lines [14], [20]. Poor de-embedding arose of mismatches of microstrip lines causing some large deviations in

the propagation constant. The Matrix-Pencil Method along combined with the De-embedding method [23] helps reducing these errors and enhances the characterization of fabric substrates. Also, application of this method, resulted in the knowledge of electrotextile`s effect on the effective permittivity of the substrate in comparison with copper.

At first, the measured S-parameters of the long and short microstrip lines are converted to T-parameters (transfer cascade matrix). If you consider the two port network Figure 2.2 and Figure 2.3; The T-parameter matrix is related to the incident and reflected waves by:

$$\begin{pmatrix} b_1 \\ a_1 \end{pmatrix} = \begin{pmatrix} T_{11} & T_{12} \\ T_{21} & T_{22} \end{pmatrix} \begin{pmatrix} a_2 \\ b_2 \end{pmatrix} \tag{5.1}$$

The advantage of T-parameters over S-parameters is that they allow cascading of two or more two-port networks by multiplying the associated individual T-parameter matrices. The conversion of S-parameters to so-called T-parameters follows from the relations [24]:

$$T_{11} = \frac{-det(S)}{S_{21}} \tag{5.2}$$

$$T_{12} = \frac{S_{11}}{S_{21}} \tag{5.3}$$

$$T_{21} = \frac{-S_{22}}{S_{21}} \tag{5.4}$$

$$T_{22} = \frac{1}{S_{21}} \tag{5.5}$$

Where *det(S)* represents the determinant of the scattering matrix.

Two microstrip lines length l_2 and another is l_1 where $l_2 > l_1$ is shown in the Figure 5.1. S_A and S_B are coax-microstrip line transition and S_L represents an ideal lossy transmission line of length l_2- l_1.
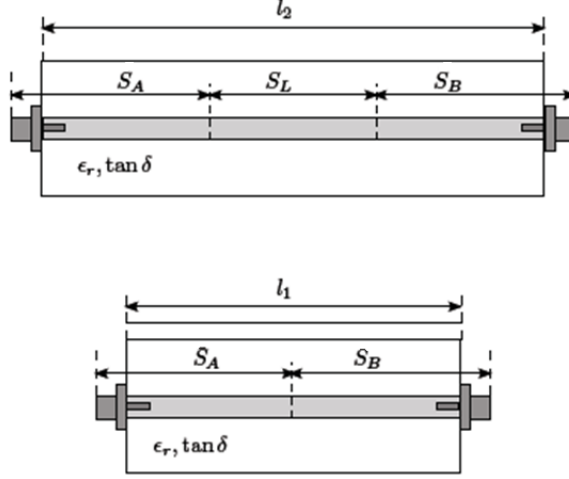
Figure 5.1: De-embedding $l_1 \, l_2$ [24].

Using the relations (5.2) to (5.5) we convert the measured scattering parameters of the long microstrip line into the transfer scattering parameters, hence we can write:

$$T_T = T_A . T_L . T_B \tag{5.6}$$

$$T_D = T_A . T_B \tag{5.7}$$

Where T_A, T_B are coax-to-microstrip discontinuities, T_L is lossy transmission line with $\Delta l = l_2 - l_1$ and T_T, T_D are corresponded to their counterpart S-parameters.

We define:

$$T = T_T . T_D^{-1} \tag{5.8}$$

Solving the T_B of (5.6) multiplying the inverse of (5.7), we get:

$$T.T_A = T_A . T_L \tag{5.9}$$

Given that T_L is diagonal, by the eigenvalue equation, the propagation factor is determined as:

$$e^{\pm \gamma \Delta l} = \frac{Tr(T) \pm \sqrt{(Tr(T))^2 - 4\Delta(T)}}{2} \tag{5.10}$$

$Tr(T)$ is trace of T and $\Delta(T)$ is equal to one due to the symmetry and reciprocity. Hence, we have two values for propagation factor and we chose the one that satisfies the fact $\left| e^{\pm \gamma \Delta l} \right| < 1$. From this value we extract complex propagation constant and from the complex propagation constant we extract effective permittivity and loss tangent values as follows;

Replacing *z=Tr (T)/2* in the (5.12) results in:

$$\gamma = \frac{\ln(z \pm \sqrt{(z^2-1)})}{\Delta l} \qquad \textbf{(5.11)}$$

After some strict mathematical operations, complex propagation constant (5.11), attenuation constant and phase constant are obtained. For obtained β, we can conclude effective permittivity:

$$\varepsilon_{r,eff} = \left(\frac{\beta}{k_0}\right)^2 \qquad \textbf{(5.12)}$$

The effective permittivity is extracted by the latter equation and in order to extract the relative permittivity ε_r of the substrate we apply inverse engineering method using Linecalc program of Agilent Technologies.

We define substrate height, microstrip line width and frequency. Then, we optimize ε_r in order to find an equal $\varepsilon_{r,eff}$ as extracted by means of the two line method. But what we do is the opposite way and we change the value of relative permittivity to reach the obtained value of effective relative permittivity.

Finally, Loss Tangent $\tan \delta$ is obtained from Formula below:

$$\tan \delta \approx 0.0366 \frac{\alpha_d \, \lambda_0 \, \sqrt{\varepsilon_{r,eff}}}{\varepsilon_r(\varepsilon_{r,eff} - 1)} (\varepsilon_r - 1) \qquad \textbf{(5.13)}$$

λ_0 is wavelength and $\alpha_d \approx \alpha$.

Relation (5.13) , satisfies till $\alpha_d >> \alpha_c$.

Briefly, the method called de-embedding extracts the complex propagation constant and from this, we obtain phase constant β and attenuation constant α. Afterwards, effective relative permittivity $\varepsilon_{r,eff}$ is calculated having phase constant β and by means of inverse engineering we obtain permittivity ε_r .Finally, all obtained parameters are used to calculate loss tangent $\tan \delta$.

5.1.1 Measurements

In this work, we characterize two different substrates, Azurri and cotton, and in order to test the repeatability of the method five different microstrip line pairs were fabricated from Flectron plus one pair of each out of copper.

For the measurement, firstly, we calibrate the network analyzer of Agilent Technologies by means of calibration tool using an Agilent`s Electronic Calibration Module as shown in the Figure 3.6 and Figure 3.7, secondly, as depicted in Figure 5.2, we connect the microstrip line to the fixed measurement cables which ensure mechanical stability of the microstrip line during measurements and minimizes the torque on the fragile coax-to-microstrip transition. Figure 5.3 shows the magnitude and phase of the propagation constant and the effective permittivity and loss tangent calculated using method above. Magnitude and phase of the propagation constant obtained using the so-called method and proceeding, loss tangent and effective permittivity extracted from the magnitude and phase of propagation constant.
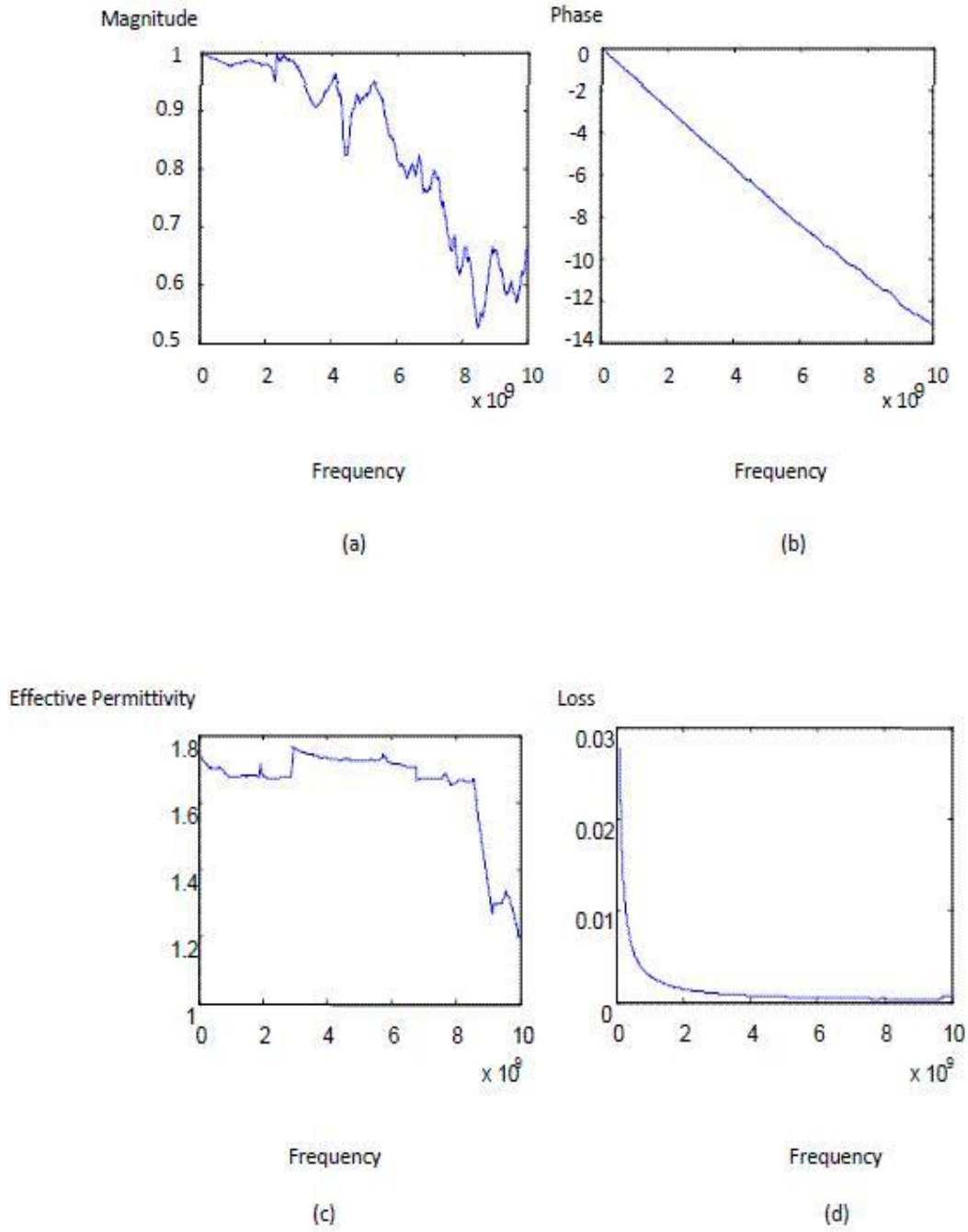

Figure 5.2: Microstrip lines measurements.

Figure 5.3: (a) Magnitude, (b) Phase of the propagation constant and the (c) Effective Permittivity and (d) Loss tangent

5.2 Inverse Antenna Method

In this part description and application of the inverse antenna method is explained along with the results.

5.2.1 Inverse problem

For the fixed antenna geometry, resonance frequency f_r is only affected by relative permittivity ε_r. For the remaining unknown parameters, loss tangent *tanδ* and conductivity σ, there are no simple relations showing the dependency of them on antenna efficiency e_{cd} and bandwidth BW. Also, antenna efficiency e_{cd} and BW are affected by ε_r of the substrate. Therefore, the inverse characterization problem presented here uses an integral equation technique solved by the Method of Moments as implemented in Momentum from Agilent Technologies.

By using this method the complex permittivity of the substrate and conductivity of the electrotextile are extracted by fitting simulated data onto measured textile antenna performances. The outputs of the simulation model are the reflection coefficient and antenna efficiency at the resonance frequency, which are then compared to the measured data in order to calculate the error functions. Then, inverse problem is converted into a forward optimization problem by minimizing an error function. Proceeding, Surrogate-based optimization technique is used in order to increase the accuracy of the method by minimizing the error function and extracting the unknown electromagnetic properties. As it is unfeasible to make a distinction between conductor losses and dielectric losses in antenna, a two-step characterization process is presented. First, the optimization process is applied to copper based textile antennas, yielding permittivity and loss tangent of the substrate. Second the optimization process is applied to electrotextile based textile antennas, resulting in the corrected permittivity of the textile substrate and the extracted effective conductivity of the electrotextile [25].

5.2.2 Surrogate modeling (SUMO) toolbox
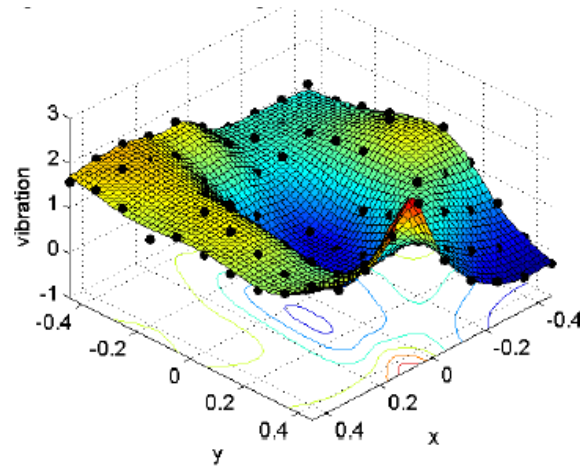
Figure 5.4: Example of SUMO Toolbox Kriging Model [27].

SUMO toolbox is a MATLAB toolbox which is used to solve inverse problem. It constructs a surrogate based model on the given data samples as depicted in Figure 5.4.The samples are well chosen points as they are chosen by optimization algorithm. This is done by building 24 initial samples which 4 are corners and the model stops building when 70 samples has been reached [26]. In Figure 5.5, you can see a clear description of SUMO toolbox function:

Figure 5.5: SUMO Toolbox functioning [26].

As the first step for SUMO toolbox before running, we have to set the permittivity, loss tangent limitation values for the Copper based antennas and in the second step where the loss tangent is extracted from step one, we set the loss tangent constant for the Flectron based antennas and we arrange the limitations for permittivity and conductivity to get the optimum point of conductivity.

5.2.3 Mean error function applied to the antennas

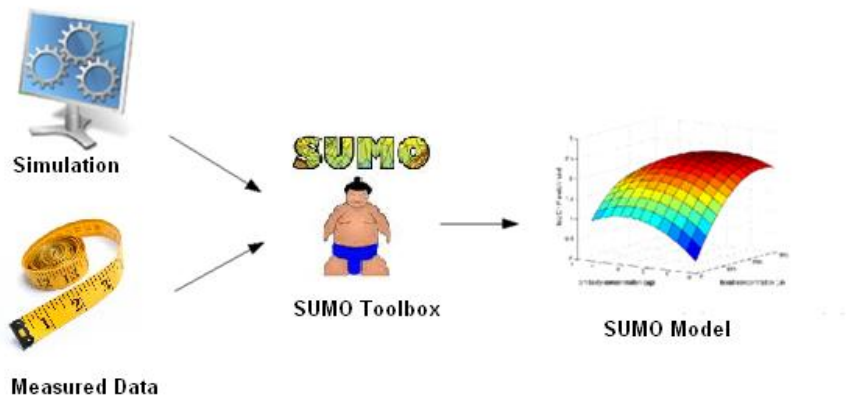SUMO toolbox `s result of Kriging model is three dimensional model where the z-axis is always defined as MSE standing for mean error function and according to the name, it is the mean value of the calculated error between the simulation results and measurement results , so defined as:

$$\text{MSE} = a_1 \frac{1}{n} \sum_{i=1}^{n} w_i \left(\left| S_{11,i} \right|^{dB} - \left| \widetilde{S_{11,l}} \right|^{dB} \right)^2 + a_2 \left| e_{cd,fr,s} - \widetilde{e_{cd,fr,m}} \right| \tag{5.14}$$

Where ~ denotes the measured data; a_1, a_2 are weighting factors and initially are one but for changing the contribution of any part, they may vary.

5.2.4 Results for antenna

Obtained results using above method is shown in this part.These results are yielded from two kinds of antennas; cotton based antennas and Azurri based antennas.

5.2.4.1 Cotton based antenna

By optimization process here, optimum points are obtained. They are representing the best agreement between simulated and measured results and showing the perfect performance of the surrogate based optimization process to optimize the error function in a relatively few numbers of evaluations. The first experiment is copper cotton antenna where we obtain MSE for given range of permittivity for [1.5 2.6] interval and loss tangent in the range [0.005 0.15].

Figure 5.6: Final Kriging surrogate model based on error function MSE in step 1 of the characterization process. Material: cotton, copper.

Table 5.1: Cotton Based Antenna Results

Antenna Type	Permittivity	Loss tangent	MSE
cotton_Copper	1.6041	0.0089	7.2248

Antenna Type	Permittivity	Conductivity(S/m)	MSE
cotton_Flectron 1	1.7028	659990	0.4976
cotton _Flectron 2	1.6842	616780	2.1777
cotton _Flectron 3	1.7164	682950	2.8348
cotton _Flectron 4	1.7204	692920	2.3614
cotton _Flectron 5	1.6678	572980	0.6569

Initially, target is obtaining the value of loss tangent.Then, we use the yielded value of loss tangent in second step of optimization of Flectron cotton antennas. In this step, we repeat the optimization process for five similar antennas where the given inputs are permittivity in the range of [1.5 2.6] and conductivity in the range of [5000 5000000]. Next is working on optimizing the conductivity for the Flectron.
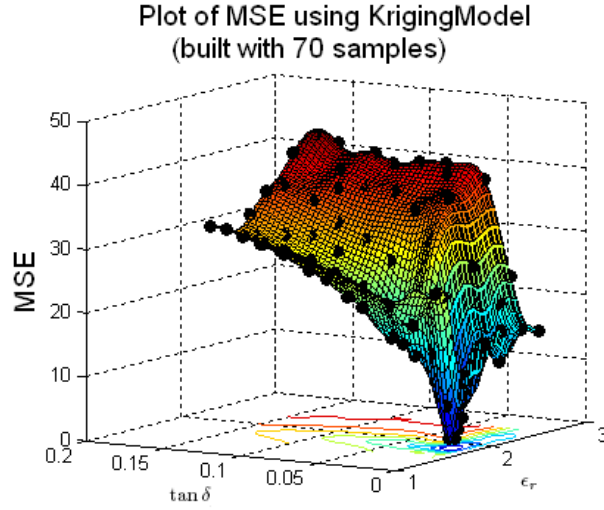
Figure 5.7: Final Kriging surrogate model based on error function MSE in step 2 of thecharacterization process. Material: cotton, Flectron.

Figure 5.6 represents the final Kriging model of cotton copper antenna where the minimum MSE can be seen clearly. This point is the optimum point which is is depicted in Table 5.1 shows the best fit between the simulated and measured results. The obtained loss tangent of this optimum point will be used as the constant input in the second step for cotton Flectron antennas. Final surrogate Kriging model of cotton Flectron is shown in Figure 5.7.

In second step, in addition of loss tangent, other two inputs are relative permittivity and conductivity. As Figure 5.7 one can see the minimum point of MSE where demonstrates the optimum point of fitted simulated and measured results. The goal of this step is to optimize the conductivity of the Flectron based antennas. Optimum values for Flectron based antennas are also depicted in Table 5.1.

5.2.4.2 Azurri based antenna

We repeat the latter operation to Azurri based antenna where the optimization initial range of permittivity is [1 1.5] and loss tangent is [0.0001 0.05], respectively. Repeatedly, loss tangent is obtained from copper Azurri antenna optimization and then this value is applied as a constant input in optimization of five Flectron based antennas. In addition, the permittivity in this step is in the range of [1 1.5] and conductivity is in the range of [5000   5000000].So, for Azurri based antennas we follow the same steps which we used in cotton based antennas. In other word, extracted loss tangent value from copper based microstripline is used in the next step to optimize the the conductivity of the electrotextile.
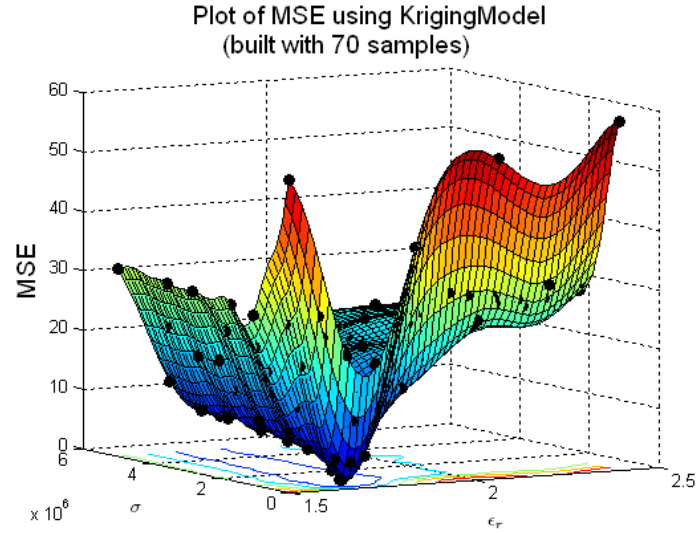

Figure 5.8: Final Kriging surrogate model based on error function MSE in step 1 of the characterization process. Material: Azurri, copper.

Table 5.2: Azurri Based Antenna Results

Antenna Type	Permittivity	Loss tangent	MSE
Azurri_Copper	1.0738	0.0076	0.5904

Antenna Type and Number	Permittivity	Conductivity(S/m)	MSE
Azurri_Flectron 1	1.0571	872380	6.4013
Azurri_Flectron 2	1.1580	481740	3.6380
Azurri_Flectron 3	1.1053	310530	7.2987
Azurri_Flectron 4	1.1369	518900	5.6703
Azurri_Flectron 5	1.1177	370250	3.1484

Figure 5.8 represents the final Kriging model of Azurri copper antenna where the minimum MSE can be seen. This point is the optimum point which is depicted in Table 5.2, shows the best fit between the simulated and measured results. The obtained loss tangent of this optimum point will be used as the constant input in the second step for Azurri Flectron antennas. Final surrogate Kriging model of cotton Flectron is shown in Figure 5.9.

In second step, in addition of loss tangent, other two inputs are relative permittivity and conductivity. Minimum point of MSE can be seen in Figure 5.9 where this point demonstrates the optimum point of fitted simulated and measured results. The goal of this step is to optimize the conductivity of the Flectron based antennas. Optimum values for Flectron based antennas are also depicted in Table 5.2.
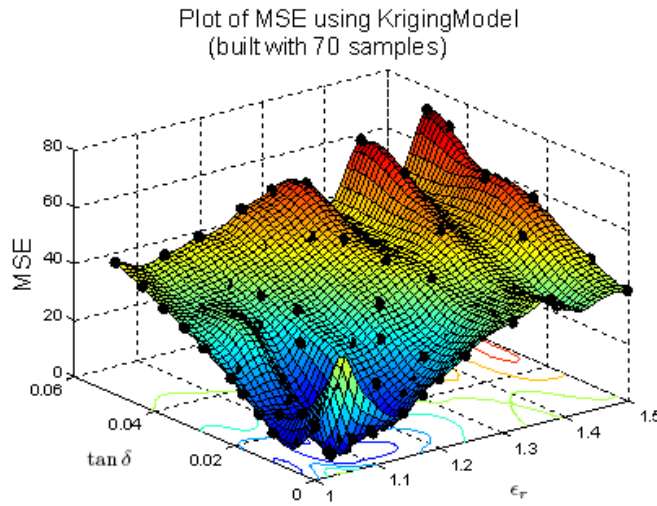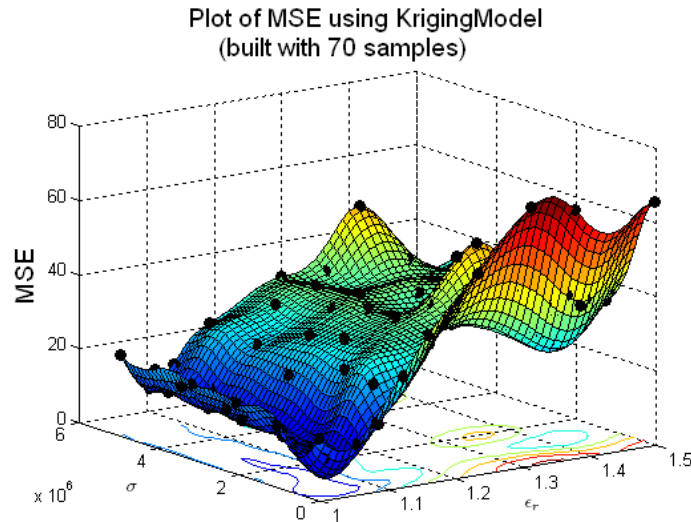

Figure 5.9: Final Kriging surrogate model based on error function MSE in step 2 of the characterization process. Material: Azurri, Flectron.

5.4.2.3 Conclusion

According to the results of Tables 5.1 and 5.2 yielded from characterization process and comparing the conductivity colum of both Tables, it can be mentioned that the stability of conductivity in the cotton based antennas is more outstanding than Azurri based antennas. Furthermore, by performing these experiments on five samples each, we could conclude in the repeatability of the results.

6. DE-EMBEDDING METHOD AND SURROGATE BASED OPTIMIZATION COMBINATION

6.1 Preview

Clearly, characterization of the electrotextile microstrip lines is as important as textile antennas characterization.Therefore, investigating on this process needs more consideration. This characterization method is as similar as the methods described in the previous sections where combination of two methods took place. So that, two microstrip lines De-embedding method applied along with the surrogate optimization method in order to optimize the characteristics of electrotextile microstrip lines. As mentioned earlier, by de-embedding the complex propagation constant is extracted and from this, we obtain phase constant β and attenuation constant α. Afterwards, effective relative permittivity $\varepsilon_{r,eff}$ is calculated having phase constant β and we obtain relative permittivity ε_r .Finally, attenuation constant α is used to obtain loss tangent $tan\,\delta$.

In this research, firstly De-embedding method is used to extract complex propagation constant of the measured S-parameters and then simulated S-parameters, respectively. Secondly, surrogate-based optimization process implemented in SUMO toolbox is applied for minimizing the defined error function. Optimization process is performed on textile microstrip lines with copper conductive material which results in finding the permittivity and loss tangent of the substrate. Next, optimization process is performed on electrotextile based textile microstrip lines to obtain permittivity and effective conductivity of the substrate.

It is of importance to mention that this combination of de-embedding and surrogate based optimization methods applied to two microstrip lines with different lengths in order to optimize their electromagnetical characteristics is being used and researched for the very first time. Although, this novel method is applied to two different materials, cotton and Azurri , further experiments on more various materials is of

need in order to reach to the general,comprehensive and applicable method to be used.

6.2 Fabrication And Measurement

As mentioned previously, twelve microstrip lines are fabricated as shown in Figure 4.3(b).Half of them are fabricated from cotton which conductor of copper is used for one and other five are from Flectron as for conductor. The substrate of other half are from Azurri which similarly, the conductor of one is copper and the rest are from Flectron. The dimensions of fabricated microstrip lines are depicted in Table 4.3 and Table 4.4.

Later, the products` S-parameters are measured using Agilent Technologies` network analyzer in the frequency range of 1-9 GHz.

6.3 Mean Error Function Applied To The Microstrip Lines

Kriging model result of SUMO toolbox is three dimensional model where the z-axis is always defined as MSE standing for mean error function and according to the name, it is the mean value of the calculated error between the simulation results and measurement results, MSE function is defined as:

$$\text{MSE} = w_1 \text{MSE}_{\text{mag}} + w_2 \text{MSE}_{\text{phase}} = w_1 \frac{1}{n} \sum_{i=1}^{n} \left(\left| \left| e_{m,i}^{-\gamma \Delta l} \right| - \left| e_{s,i}^{-\gamma \Delta l} \right| \right| \right)^2 +$$

$$w_2 \frac{1}{n} \sum_{i=1}^{n} \left(\left| \angle \left| e_{m,i}^{-\gamma \Delta l} \right| - \angle \left| e_{s,i}^{-\gamma \Delta l} \right| \right| \right)^2 \qquad \textbf{(6.1)}$$

Where w_1, w_2 are weighting factor, n is the number of frequency points. $\left| e_m^{-\gamma \Delta l} \right|$ is the magnitude of propagation constant and $\angle \left| e_m^{-\gamma \Delta l} \right|$ is the phase of propagation constant and s and m subscripts are representing simulation and measurement, respectively.

6.4 Results For Microstrip Lines

6.4.1 Cotton based microstrip lines

By optimization process here, optimum points are obtained. They are representing the best agreement between simulated and measured results and showing the perfect performance of the surrogate based optimization process to optimize the error function in a relatively few numbers of evaluations. The first experiment is copper cotton microstrip lines where we obtain MSE for given range of permittivity for [1.4 1.8] interval and loss tangent in the range [0.005 0.15].
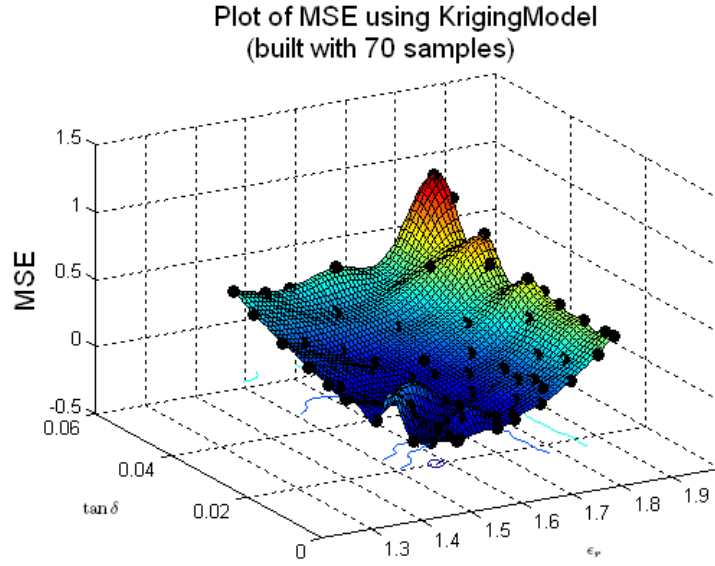

Figure 6.1: Final Kriging surrogate model based on error function MSE in step 1 of the characterization process. Material: cotton, copper.

In advance, the optimum value of the loss tangent is found. Then, we use the yielded value of loss tangent in second step of optimization of Flectron cotton microstrip lines. In this step, we repeat the optimization process for five similar microstrip lines where the given inputs are permittivity in the range of [1.5 2.6] and conductivity in the range of [5000 5000000]. Next is working on optimizing the conductivity for the Flectron based antennas. Figure 6.1 and Figure 6.2 show the cotton based microstrip line Kriging model and Flectron based microstrip line Kriging model, respectively. The optimums points are shown at Table 6.1.

Table 6.1: Cotton based microstrip lines results

Microstrip Line Type	Permittivity	Loss tangent	MSE
cotton_copper	1.4836	0.0082	3.0926

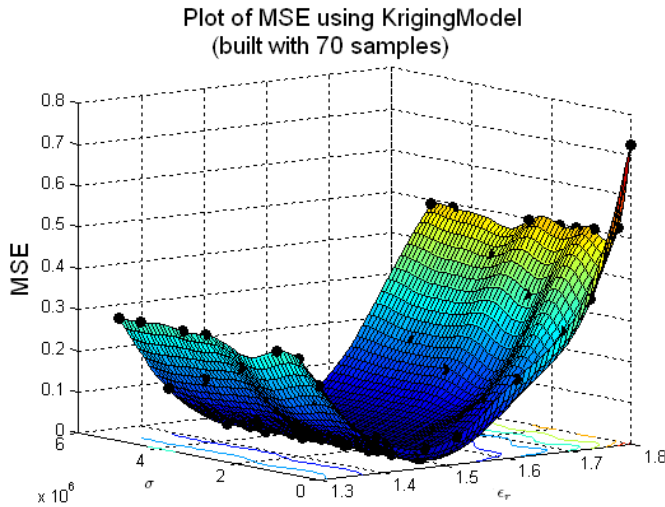| Microstrip Line Type	Permittivity	Conductivity(S/m)	MSE
cotton_Flectron 1	1.529	926319	0.0011
cotton _Flectron 2	1.4788	700710	0.0009
cotton _Flectron 3	1.5066	642450	0.0022
cotton _Flectron 4	1.4814	469320	0.0054
cotton _Flectron 5	1.4848	689740	0.0059

Figure 6.2: Final Kriging surrogate model based on error function MSE in step 1 of the characterization process. Material: cotton, Flectron.

Though, optimum point for cotton based microstrip line can be seen in the Figure 6.1, obtained optimum point for Flectron based microstrip cannot be seen easily as shown in Figure 6.2.Actually, Flectron based microstrip lines have a valley of minimums instead of clear-cut minimum point. Even copper based microstrip line Kriging model was valley shaped where we could get Figure 6.1 by limiting the permittivity level [1.4 1.8].

6.4.2 Azurri based microstrip lines

We repeat the latter operation to Azurri based microstrip lines where the optimization initial range for permittivity is [1 1.5] and loss tangent is [0.0001 0.05], respectively. Repeatedly, loss tangent is obtained from copper microstrip line optimization and then this value is applied as a constant input into the optimization of five Flectron based microstrip lines. In addition, the permittivity in this step is in the range of [1 1.5] and conductivity is in the range of [5000 5000000].So, for Azurri based microstrip lines follow the same steps applied in cotton based microstriplines. Meaning that, extracted loss tangent value from copper based microstripline is used in the next step to optimize the conductivity of the electrotextile.
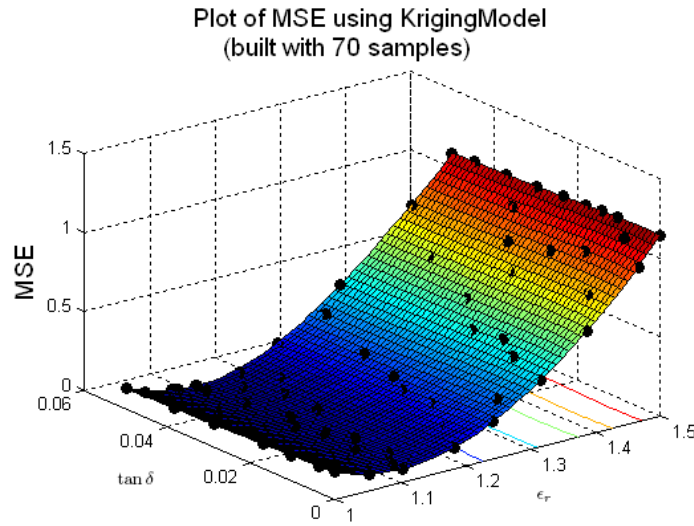

Figure 6.3: Final Kriging surrogate model based on error function MSE in step 1 of the characterization process. Material: Azurri, copper.

Microstrip Line Type	Permittivity	Loss tangent	MSE
Azurri_copper	1.1074	0.05	0.0326

MIcrostrip Line Type	Permittivity	Conductivity(S/m)	MSE
Azurri_Flectron 1	1.1491	3843321	0.0214
Azurri _Flectron 2	1.0028	487869	0.1025
Azurri _Flectron 3	1.2397	2582986	0.0302
Azurri _Flectron 4	1.0236	4687813	0.0155
Azurri _Flectron 5	1.1703	2978098	0.0188

Table 6.2: Azurri based microstrip lines results.

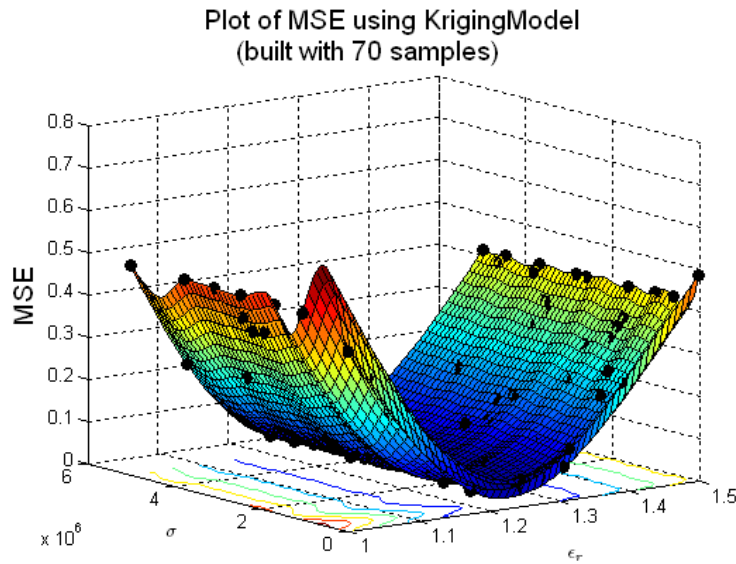Plot of MSE using KrigingModel (built with 70 samples)

Figure 6.4: Final Kriging surrogate model based on error function MSE in step 1 of the characterization process. Material: Azurri,Flectron.

Obtained Kriging model for copper based microstrip line and Flectron based microstrip line is shown in Figure 6.3 and Figure 6.4, respectively. Also, related optimum points are depicted in Table 6.2.Figures of Azurri based microstrip lines either with copper or with Flectron are valley shaped and despite of abundant efforts in limiting the permittivity, loss tangent and conductivity or changing the weighting factors, representing the clear cut optimum points was not probable. However, the optimum points of Azurri based microstrip lines are depicted in Table 6.2.

6.4.3 Conclusion

According to the results of Tables 6.1 and 6.2, yielded from combined characterization process and comparing the conductivity colum of both Tables, it can be mentioned that the stability of conductivity in the cotton based microstrip lines is more balanced than Azurri based microstrip lines. Furthurmore, by performing these experiments on five samples each, we could conclude in the repeatability of the results.

Similarities in permittivity ,loss tangent and conductivity among the cotton based microstrip lines and antenna results has been reached.Though, still needs some accuracy measures. In other side,among Azurri based microstrip lines and antennas,only the permittivity values were relatively similar and there was a rather large discrepancy in loss tangent values.Also,unstability in conductivity range of Azurri based microstrip lines are more than that in Azurri based antennas.

7. CONCLUSIONS AND FUTURE WORK

The ultimate goal of this research was to characterize the electromagnetic properties of electrotextile based conductive materials in order to development in wearable antennas and microstrip lines. This is done by the usage of two methods; Inverse antenna problem and De-embedding method applied for microstrip lines.

In Inverse antenna problem study;

Method applied on two types of substrates cotton and Azurri. Due to the inevitability on distinction between conductor losses and substrate losses, copper and Flectron are used as the conductor in both antennas in order to distinct the losses.At the first step, loss tangent extracted from copper based antennas where extracting the conductivity took place in the second step.

By this method, more stable conductivity reached in the cotton based antennas rather Azurri based antennas.

Via performing this method on five samples of each antenna, repeatability of the results has been studied.

In De-embedding method study;

Applying the method on two microstrip lines with different lengths, complex propagation constant of the ideal lossy transmission line is extracted where from that relative permittivity and loss tangent of the substrate can be calculated.

In the combined method of De-embedding and SBO study;

De-embedding is applied for measured and simulated data along with the surrogate based optimization implemented in SUMO toolbox in order to obtain optimum points.

Repeatedly, this is done for same materials for antennas and in the same quantity. Also, obtaining the electrotextile microstrip lines are two folded as like antennas.

There are similarities in permittivity ,loss tangent and conductivity among the cotton based microstrip lines and antenna results.

In the other hand,among Azurri based microstrip lines and antennas,only the permittivity values were relatively similar and there was a rather large discrepancy in loss tangent values.Also,unstability in conductivity range of Azurri based microstrip lines are more than that in Azurri based antennas.

FUTURE WORK

In this thesis, Inverse antenna problem is performed on only two materials cotton and Azurri. Further studies on other fabrics can be done.

Also, de-embedding method has been performed on only two kinds of fabrics and further studies on different fabrics can be done.

The combination of de-embedding method and SBO results have some deviations and still need some more accuracy measures to be performed on, in order to yield more similar results with their antenna counterpart .

Meanwhile, latter method can be performed on different microstriplines with different fabrics as substrate.

REFERENCES

[1]   **P. Salonen, L. Sydanheimo, M. Keskilammi, and M. Kivikoski,** "A small planar inverted-F antenna for wearable applications," in *Wearable Computers, 1999. Digest of Papers. The Third International Symposium on*, 1999, pp. 95 –100.

[2]   **Carla Hartler** "Carla Hartler PhD Thesis" Gent University.

[3]   **"Samlab | Multi-Parametric Sensing Platform on Flexible Substrate."** [Online]. Available: http://samlab.epfl.ch/page-74173-en.html.

[4]   **P. J. Massey**, "Mobile phone fabric antennas integrated within clothing," in *Antennas and Propagation, 2001. Eleventh International Conference on (IEE Conf. Publ. No. 480)*, 2001, pp. 344 –347 vol.1.

[5]   **Frederick Declercq**, "Frederick Declercq PhD thesis" Gent University.

[6]   **"ESA Portal - The washable wearable antenna,"** 29-Sep-2011. [Online]. Available: http://www.esa.int/esaCP/SEMO3L6UXSG_index_0.html

[7]   **A. Dierck, T. De Keulenaer, F. Declercq, and H. Rogier,** "A wearable active GPS antenna for application in smart textiles," *Proceedings of the 32nd ESA Antenna Workshop on Antennas for Space Applications*, 2010. [Online]. Available: https://biblio.ugent.be/publication/1163211.

[8]   **T. F. Kennedy, P. W. Fink, A. W. Chu, and G. F. Studor,** "POTENTIAL SPACE APPLICATIONS FOR BODY-CENTRIC WIRELESS AND E-TEXTILE ANTENNAS," in *Antennas and Propagation for Body-Centric Wireless Communications, 2007 IET Seminar on*, 2007, pp. 77 –83.

[9]   **Prof.H.Rogier**, *Antennas and Propagation Course Book*. Gent University , 2007.

[10]   **Peter Joseph Bevelacqua**, "www.antenna-theory.com." .

[11]   **P. Bhartia, I. Bahl, R. Garg, and A. Ittipiboon,** *Microstrip Antenna Design Handbook*. Artech House Publishers, 2001.

[12]   **"Radiation pattern for a dual band microstrip patch antenna - The RadioReference.com Forums."** [Online]. Available: http://forums.radioreference.com/scanner-receiver-antennas/211972-radiation-pattern-dual-band-microstrip-patch-antenna.html.

[13]   **H. A. Wheeler,** "The Radiansphere around a Small Antenna," *Proceedings of the IRE*, vol. 47, no. 8, pp. 1325 –1331, Aug. 1959.

[14]   **D. M. Pozar and B. Kaufman,** "Comparison of three methods for the measurement of printed antenna efficiency," *Antennas and Propagation, IEEE Transactions on*, vol. 36, no. 1, pp. 136 –139, Jan. 1988.

[15]   **E. Newman, P. Bohley, and C. Walter,** "Two methods for the measurement of antenna efficiency," *Antennas and Propagation, IEEE Transactions on*, vol. 23, no. 4, pp. 457 – 461, Jul. 1975.

[16]   **R. H. Johnston and J. G. McRory,** "An improved small antenna radiation-efficiency measurement method," *Antennas and Propagation Magazine, IEEE*, vol. 40, no. 5, pp. 40 –48, Oct. 1998.

[17]   **"Microstrip   Analysis/Synthesis   Calculator."**   [Online].   Available: http://mcalc.sourceforge.net/.

[18]   **J Choma & WK Chen.,** *Feedback networks: theory and circuit applications.* chapter 3 vols. World Scientific, 2007.

[19]   **D. M. Pozar,** *Microwave Engineering*, 2nd ed. Wiley, 1997.

[20]   **"Microstrip - Microwave Encyclopedia - Microwaves101.com."** [Online]. Available: http://www.microwaves101.com/encyclopedia/microstrip.cfm.

[21]   **M. D. Janezic and J. A. Jargon,** "Complex permittivity determination from propagation constant measurements," *Microwave and Guided Wave Letters, IEEE*, vol. 9, no. 2, pp. 76 –78, Feb. 1999.

[22]   **M.-Q. Lee and S. Nam,** "An accurate broadband measurement of substrate dielectric constant," *Microwave and Guided Wave Letters, IEEE*, vol. 6, no. 4, pp. 168 –170, Apr. 1996.

[23]   **F. Declercq, H. Rogier, and C. Hertleer,** "Permittivity and Loss Tangent Characterization for Garment Antennas Based on a New Matrix-Pencil Two-Line Method," *Antennas and Propagation, IEEE Transactions on*, vol. 56, no. 8, pp. 2548 –2554, Aug. 2008.

[24]   **Agilent Technologies,** "S-Parameter Design." Application Note AN 154; Agilent Technologies; p 14.

[25]   **F. Declercq, I. Couckuyt, H. Rogier, and T. Dhaene,** "Complex permittivity characterization of textile materials by means of surrogate modelling," in *Antennas and Propagation Society International Symposium (APSURSI), 2010 IEEE*, 2010, pp. 1 –4.

[26]   **"Home - SUMO Lab | SUMO - SUrrogate MOdeling Lab."** [Online]. Available: http://sumo.intec.ugent.be/.

CURRICULUM VITAE

Name Surname: Toumaj KOHANDEL GARGARI

Place and Date of Birth: Tabriz, Iran 29/06/1984

Address: Sisli, Istanbul

E-Mail: toumaj.kohandel@gmail.com

B.Sc.: Electronics Engineering , IAUT, Tabriz

M.Sc. Electronics and Telecommunications Engineering, ITU, Istanbul